indicates incorrect folding, although we know of no evidence to indicate that a correctly folded single zinc finger is capable of sequence-specific binding. Indeed, point mutations in ADR1 (7) indicated that both fingers were essential for protein activity. In addition, a peptide fragment containing three zinc fingers (*10*) has been shown to footprint DNA. Taken together, these peptide-fragment DNA-binding results might suggest that multiple fingers are required to contribute the correct number and type of base contacts for sequence-specific binding to occur, or that a single-finger domain requires a larger protein context in order to maintain the proper geometry for specific DNA binding. Further analysis of the 2D NMR spectra of the single- and double-finger peptides should allow us to determine the complete structure of this nucleic acid–binding motif, and should be an important step toward an understanding of how multiple fingers bind DNA.

REFERENCES AND NOTES

1. A. Klug and D. Rhodes, *Trends Biochem. Sci.* **12**, 464 (1987).
2. R. M. Evans and S. M. Hollenberg, *Cell* **52**, 1 (1988).
3. J. Miller, A. D. McLachlan, A. Klug, *EMBO J.* **4**, 1609 (1985).
4. R. S. Brown, C. Sander, P. Argos, *FEBS Lett.* **186**, 271 (1985).
5. C. L. Denis and E. T. Young, *Mol. Cell. Biol.* **3**, 360 (1983).
6. T. A. Hartshorne, H. Blumberg, E. T. Young, *Nature* **320**, 283 (1986).
7. H. Blumberg, A. Eisen, A. Sledziewski, D. Bader, E. T. Young, *ibid.* **328**, 443 (1987).
8. A. Eisen, W. E. Taylor, H. Blumberg, E. T. Young, unpublished results.
9. S. Thrukal, W. E. Taylor, A. Eisen, E. T. Young, unpublished results.
10. K. Nagai, Y. Nakaseko, K. Nasmyth, D. Rhodes, *Nature* **332**, 284 (1988).
11. D. Roise, S. J. Horvath, J. M. Tomich, J. H. Richards, G. Schatz, *EMBO J.* **5**, 1327 (1986).
12. M. F. Bruist, S. J. Horvath, L. E. Hood, T. A. Steitz, M. I. Simon, *Science* **235**, 777 (1987).
13. A. D. Frankel, J. M. Berg, C. O. Pabo, *Proc. Natl. Acad. Sci. U.S.A.* **84**, 4841 (1987).
14. G. P. Diakun, L. Fairall, A. Klug, *Nature* **324**, 698 (1986).
15. Spectra of the folded form of ADR1a have been obtained from 15° to 35°C. No significant temperature-dependent chemical shifts have been observed, indicating that the system is in slow exchange. Furthermore, in samples containing a mixture of unfolded and folded species (oxidized and reduced species), separate resonances were observed for each form of the peptide, again indicating slow exchange behavior.
16. C. T. Chang, C. H. C. Wu, J. T. Yang, *Anal. Biochem.* **91**, 13 (1978).
17. A. D. Frankel, D. S. Bredt, C. O. Pabo, *Science* **240**, 70 (1988).
18. M. Billeter, W. Braun, K. Wüthrich, *J. Mol. Biol.* **155**, 321 (1982).
19. R. S. Brown and P. Argos, *Nature* **324**, 215 (1986).
20. P. Y. Chou and G. D. Fasman, *Biochemistry* **13**, 222 (1974).
21. J. M. Berg, *Proc. Natl. Acad. Sci. U.S.A.* **85**, 99 (1988).
22. Abbreviations for the amino acid residues are: A, Ala; C, Cys; D, Asp; E, Glu; F, Phe; G, Gly; H, His; I, Ile; K, Lys; L, Leu; M, Met; N, Asn; P, Pro; Q, Gln; R, Arg; S, Ser; T, Thr; V, Val; W, Trp; and Y, Tyr.
23. Raw data were obtained and are shown without any curve smoothing with a resolution of 0.2 nm per data point; each data point represents the average of 40 samples. Ellipticity values at 222 nm were converted to mean molar residue ellipticity values with the equation $[\theta]222 = \theta M_r/(100Lc)$, where θ = degrees, L = cell path length (dm), c = concentration (g/ml), and M_r = mean residue molecular weight calculated from the amino acid sequence. Fraction of helix f_H was calculated as $f_H = [\theta]222/\{[\theta]^H(1 - k/n)\}$, where $[\theta]^H = -37{,}400$, $k = 2.5$, and $n = 9$ [k is the chain length dependence factor, and n is the number of residues in a typical α-helical segment (*16*)].
24. NOESY spectra have been obtained in the phase-sensitive mode with mixing times of 200, 300, 400, and 600 ms to assess the degree of spin diffusion. Spectra obtained for samples in 90% H_2O solutions were acquired with a presaturation pulse of 2.0 s.

25. We thank B. R. Reid and G. Drobny and their groups for use of NMR facilities; H. Charbonneau, S. Kumar, M. Harrylock, R. Wade, and K. Walsh for assistance with amino acid compositional analysis and for sequencing the peptide; and our colleagues D. Allison, J. Herriott, and B. M. Shapiro for their helpful comments on the manuscript.

15 June 1988; accepted 12 August 1988

Virus-Specific Splicing Inhibitor in Extracts from Cells Infected with HIV-1

DELIA GUTMAN AND CARLOS J. GOLDENBERG*

Human immunodeficiency virus type 1 (HIV-1), in contrast with most other retroviruses, encodes trans-regulatory proteins for virus gene expression. It is shown in this study, by means of an in vitro splicing system, that nuclear extracts obtained from cells infected with HIV-1 contain a factor (or factors) that specifically inhibits splicing of a synthetic SP6/HIV pre–messenger RNA (pre-mRNA)–containing donor and acceptor splice sites in the coding region for the envelope protein. It is also shown that the SP6/HIV pre-mRNA is not capable of assembly in a ribonucleoprotein complex, spliceosome, in extracts from infected cells. These findings raise the possibility that specific inhibition of pre-mRNA splicing in the envelope protein coding region by HIV-1 trans-regulatory factors might be one control mechanism for efficient production of structural viral proteins and virion assembly.

THE HUMAN IMMUNODEFICIENCY virus type 1 (HIV-1) contains, in addition to genes *gag*, *pol*, and *env*, at least five other genes termed *vif*, *vpr*, *nef*, *tat*-3, and *rev* (*1*). The *tat*-3 and *rev* genes are essential for virus expression (*2–10*), but their precise functions remain to be defined. The *tat*-3 gene codes for a protein of 86 amino acids (*9, 10*) that interacts directly or indirectly with sequences located downstream from the HIV-1 initiation site for transcription (TAR element) (*11*). Several studies with viral deletion mutants suggest that *tat*-3 is required for translation of viral mRNAs (*8, 12*); it appears to function by increasing the steady-state level of mRNA by direct transcriptional activation (*3, 13*), antitermination (*14*), or mRNA stabilization (*3–5, 15*). The product of the *rev* gene is a protein of 116 amino acids (*2, 7, 8, 10*). It may also operate at several levels, it may relieve a translational block of *gag* and *env* proteins (*7*), affecting the relative abundance of viral mRNAs (*8*), and it may also have a negative trans-regulatory role in transcription (*16*). Feinberg *et al.* (*8*) reported an abnormal pattern of HIV-1 viral mRNAs in monkey (COS) cells transfected with *rev*-defective mutants. The levels of the 9-kb (*gag/pol*) and 4.3-kb (*env*) mRNAs were very low and that of the 2-kb (*tat*-3/*rev*)

Department of Microbiology and Immunology, University of Miami School of Medicine, Miami, FL 33101.

*To whom correspondence should be addressed.

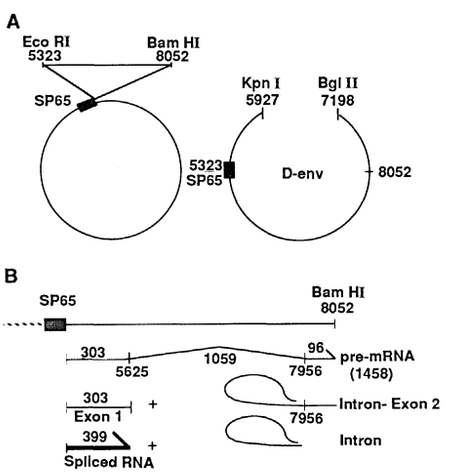

Fig. 1. Cloning of HIV-env DNA into SP65 vectors. (**A**) The HIV-1 DNA Eco RI–Bam HI fragment (nucleotides 5323 to 8052) was cloned into the SP65 vector. This DNA was isolated and sequences between Kpn I–Bgl II (5927 to 7198) were deleted. (**B**) The expected RNAs from in vitro splicing of SP65/HIV pre-mRNA transcribed from the D-env DNA linearized at the Bam HI site (line with stippled box) are schematically represented. The numbers above the lines represent the nucleotide length of the RNAs.

mRNAs was disproportionately high. They concluded that *rev* might control the extent of mRNA splicing, such that the larger mRNA species are maintained. However, a role in stabilizing the larger mRNA species was not ruled out. We demonstrate that in vitro splicing of a synthetic HIV-1 pre-mRNA, containing donor and acceptor splice sites in the *env*-coding region, is inhibited in nuclear extracts obtained from human T cells infected with HIV-1. Further analysis revealed that spliceosomes were unable to form on synthetic HIV-1 pre-mRNA in nuclear extracts obtained from HIV-1–infected cells.

To facilitate the analysis of the in vitro splicing products, we first cloned the HIV-1 DNA fragment nucleotides 5323 to 8052 [the nucleotide numbers of the HIV-1 genome were from (*4, 16a*)] into the SP65 vector (Fig. 1A). This DNA clone was isolated and intron sequences from nucleotides 5927 to 7198 were deleted to generate shorter pre-mRNAs for in vitro assays. The DNA clone (D-env) contains a donor splice site at nucleotide 5625 and an acceptor splice site at nucleotide 7956 (Fig. 1B). The expected products of the splicing reaction for this pre-mRNA are shown in Fig. 1B.

The synthetic SP6/HIV pre-mRNA was prepared from the D-env plasmid DNA digested at the Bam HI site (Fig. 1B). The ^{32}P-labeled pre-mRNAs (1458 nucleotides) were gel-purified and used as substrates for splicing reactions (*17*) in the presence of nuclear extracts from HIV-1–infected H9 cells, uninfected H9 cells, and HeLa cells. The expected RNA splicing products were detected only with nuclear extracts from uninfected H9 or HeLa cells (Fig. 2A, lanes 2 and 3). Pre-mRNA splicing was not detected with extracts obtained from HIV-1–infected H9 cells (Fig. 2A, lane 4). Titration of this extract (between 5 and 150 μg of protein) produced the same results. In contrast, the SP6/mouse insulin pre-mRNA was spliced either in HIV-1–infected or uninfected extracts (Fig. 2B). These results indi-

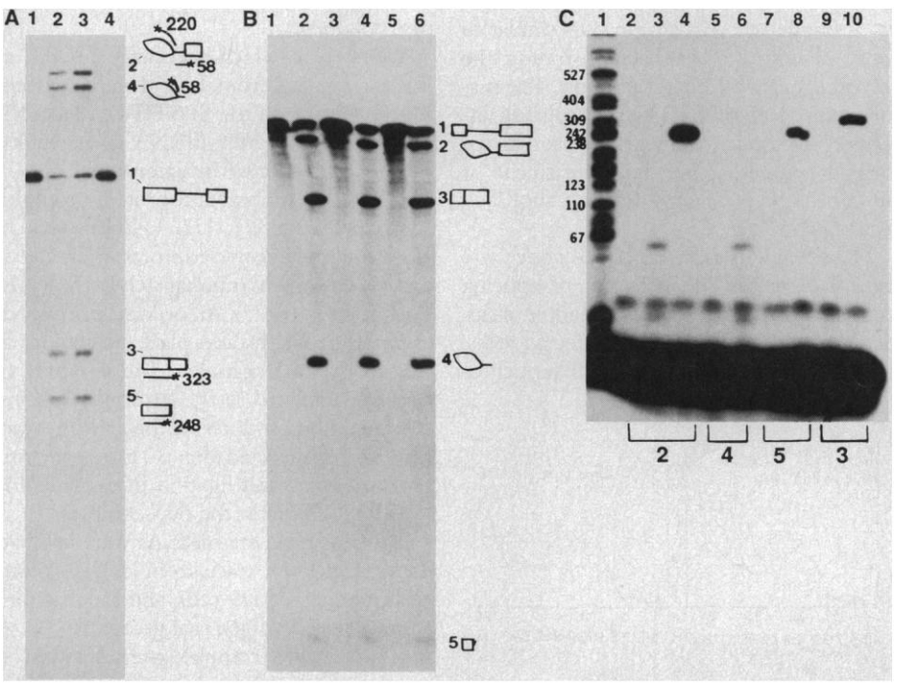

Fig. 2. Effect of nuclear extracts obtained from HIV-1–infected cells on SP6/HIV pre-mRNA splicing. The pre-mRNAs were transcribed with SP6 RNA polymerase in the presence of [^{32}P]α-GTP (guanosine triphosphate) from the D-env DNA clone linearized at the Bam HI site (Fig. 1) or the SP6/mouse insulin DNA clone linearized at the Eco RI site (*17, 28*). The pre-mRNAs were gel purified and used as substrates in splicing reactions incubated at 30°C for 90 min (*17*). The nuclear extracts were purified from HeLa cells, H9 cells uninfected or H9 infected with HIV-1 as described (*17, 28*). For a 25-μl splicing reaction, 150 μg of protein of each of the extracts was used. The RNAs were then purified and analyzed on 4% (A) or 60% (B) 8*M*-urea polyacrylamide gels. (**A**) SP6/HIV pre-mRNA incubated without HeLa cell extract (lane 1), with HeLa cell extract (lane 2), with H9 uninfected extract (lane 3), and with H9 HIV-1–infected extract (lane 4). (**B**) SP6/mouse insulin pre-mRNA incubated without extract (lanes 1, 3, and 5), with HeLa cell extract (lane 2), with H9 uninfected extract (lane 4), and with H9 HIV-1–infected extract (lane 6). (**C**) Primer-extension analysis of the RNA splicing products from the SP6/HIV pre-mRNAs generated in H9 uninfected extracts. The RNA species 2 to 5 shown in (A) (lane 3) were eluted and used as templates for reverse transcriptions (*17, 28*). The 20-bp oligonucleotide primers labeled at the 5′ end used for each of the different RNA species, as well as the expected cDNA sizes, are indicated on the right of (A). Different amounts of the purified RNA species were used for primer extensions. Therefore, the relative intensities of the cDNA bands do not represent the relative abundance of the RNA splicing products. Minus RNA species plus primers (lanes 2, 5, 7, and 9). RNA species 2 extended with a primer complementary to nucleotides 7976 to 7956, expected cDNA size, 58 nucleotides (lane 3). RNA species 2, extended with a primer complementary to nucleotides 7794 to 7774, expected cDNA size, 220 nucleotides (lane 4). Three times more RNA was used as in lane 3. RNA species 4, primer complementary to nucleotides 7936 to 7956 (lane 6). RNA species 5, primer complementary to nucleotides 5575 to 5555 (lane 8). RNA species 3, primer complementary to 7976 to 7956 (lane 10). Lane 1, PBR322 digested with MSP I 5′-end labeled with [^{32}P]adenosine triphosphate (ATP) used as markers. Sizes (in nucleotides) are indicated on the left. The RNA species used for primer extension are also indicated at the bottom of (C).

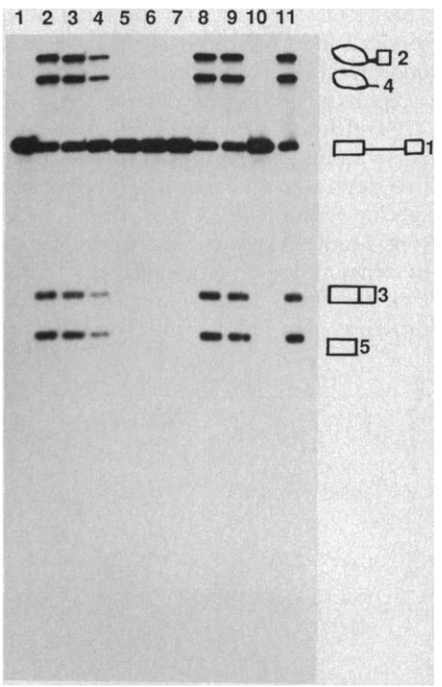

Fig. 3. Characterization and fractionation of the inhibitory splicing factor, or factors, for SP6/HIV pre-mRNAs. The nuclear extract (30 mg/ml) obtained from HIV-1–infected cells was mixed with uninfected H9 extracts for splicing reactions (inhibition assay). A 1-μl portion containing either 30 μg of bovine serum albumin (lane 2) or 5, 15, or 30 μg of protein of HIV-1 extract (lanes 3 to 5, respectively) was added to 15 μl of uninfected extracts (150 μg of protein). Splicing reactions were then carried out as described (Fig. 2). SP6/HIV pre-RNAs incubated without extract (lane 1). The nuclear extract from HIV-1–infected cells was fractionated on a blue-dextran agarose column and the eluted fraction was applied to a DEAE-Sepharose column (*29*). The column fractions, 10 μg of protein, were mixed with uninfected extracts as described above (inhibition assay). Blue-dextran agarose column, flow-through fraction (lane 6), eluted (0.6*M* KCl) fraction (lane 7). DEAE-Sepharose column, flow-through, 0.1*M* KCl (lane 8). Eluted fractions 0.2, 0.3, and 0.5*M* KCl (lanes 9 to 11, respectively). The RNA species 1 to 5 are indicated on the right.

cate that HIV-1–infected cells contain a factor (or factors) that specifically inhibits the splicing of the intron in the envelope-coding region: splice donor at nucleotide 5625 and splice acceptor at nucleotide 7956.

The characterization of each of the SP6/mouse insulin RNA splicing products was previously reported (*17*). Primer-extension analysis of the gel-purified splicing products obtained from reactions with SP6/HIV pre-mRNAs and uninfected H9 extracts generated the expected cDNA sizes for each of the different RNA species (Fig. 2C). The RNA species 2 generated, with a 20-bp oligonucleotide primer, a 58-nucleotide cDNA, indicating the presence of a structure located at 38 nucleotides from the acceptor splice site that blocks the reverse transcriptase. This result suggests that the lariat RNA species 2 and 4 contained a branching nucleotide located at 38 nucleotides from the acceptor splice site (adenine at nucleotide 7994) that was generated during the splicing reaction of HIV pre-mRNAs. Moreover, it was expected that RNA species from splicing reactions in a lariat configuration (Fig. 2A, RNA species 2 and 4) will migrate in denaturing polyacrylamide gels slower than the linear forms (*18*). We conclude therefore, that splicing of SP6/HIV pre-mRNAs occurs in uninfected extracts by formation of RNA lariat intermediates, as reported for many other eukaryotic genes (*17–19*).

The inhibitory effect of the HIV-1–infected extracts was further characterized by mixing experiments. Nuclear extracts obtained from uninfected H9 cells that were able to splice SP6/HIV pre-mRNAs were mixed with an increasing concentration of extracts obtained from HIV-1–infected cells; the inhibitory factor acts in a dose-dependent manner (Fig. 3, lanes 2 to 5). In contrast, no effect on splicing of SP6/mouse insulin pre-mRNAs was observed by mixing nuclear extracts obtained from HIV-1–infected cells with uninfected extracts. Eight different nuclear extracts prepared from HIV-1–infected or uninfected cells gave results similar to those described above, demonstrating the reproducibility of the observation. The major component of this specific splicing inhibitory factor is most likely a protein (or proteins), since either heat treatment at 65°C or repeated freeze-thawing abolished its activity.

The inhibition assay described above was used to test for the presence of splicing inhibitory factor during fractionation of nuclear extracts from HIV-1–infected cells. The fractions eluted from the different chromatographic columns (equivalent amounts to 30 μg of protein of nuclear extract) were mixed with nuclear extracts from uninfected H9 cells and used for splicing reactions of SP6/HIV pre-mRNAs. The inhibitory activity was initially fractionated by a blue-dextran agarose chromatography. The activity was recovered in the flow-through fraction and in the 0.6*M* KCl eluted fraction (Fig. 3, lanes 6 and 7). The eluted fraction from the blue-dextran agarose column was further fractionated on a DEAE-Sepharose column, and the activity recovered in the 0.3*M* KCl eluted fraction (Fig. 3, lane 10). The overall enrichment of the inhibitory splicing factor (or factors) from the nuclear extract was about 160-fold (8-fold by the blue-dextran column and 20-fold by the DEAE-Sepharose column).

The step at which the factor present in nuclear extracts from HIV-1–infected cells blocks splicing of the SP6/HIV pre-mRNA was investigated. Pre-mRNA is assembled during the splicing reaction into a 60*S* (spliceosome) ribonucleoprotein complex (*18*) containing U1, U2, U4/U6, and U5 small nuclear ribonucleoproteins (snRNPs) and heterogenous nuclear RNP (hnRNP) proteins (*17, 19–23*). An ordered pathway of assembly probably takes place during formation of the 60*S* complex. The assembly of the 60*S* is related to the lag of the splicing reaction. The products of the splicing reaction are first detected after 30 min of incubation. Cleavage and ligation of pre-mRNAs (splicing) occurs in the 60*S* complex.

The SP6/HIV pre-mRNAs were incubated with nuclear extracts from HIV-1–infected or uninfected H9 cells, and the reactions were analyzed on glycerol gradients (*17*). A 60*S* and a 40*S* complex were detected in reactions with uninfected extracts (Fig. 4A). In contrast, only a 40*S* complex was detected in reactions with infected extracts (Fig. 4B). The RNAs were extracted from each of the glycerol gradient fractions and analyzed on denaturing polyacrylamide gels. The 60*S* complex formed with uninfected extracts contained the products of the splicing reaction (Fig. 4A). In contrast, in reactions with HIV-1–infected extracts the SP6/HIV pre-mRNA was detected only in a 40*S* complex. The control SP6/mouse insulin pre-mRNA was able to generate a 60*S* complex containing the products of the splicing reaction in either uninfected or HIV-1–infected extracts (Fig. 4, C and D). These results indicate that blocking of splicing occurred at the level of spliceosome assembly, specifically with SP6/HIV pre-mRNAs in extracts obtained from HIV-infected cells.

The experiments presented here demonstrate the presence of a factor, or factors, in HIV-1–infected cells that specifically inhib-

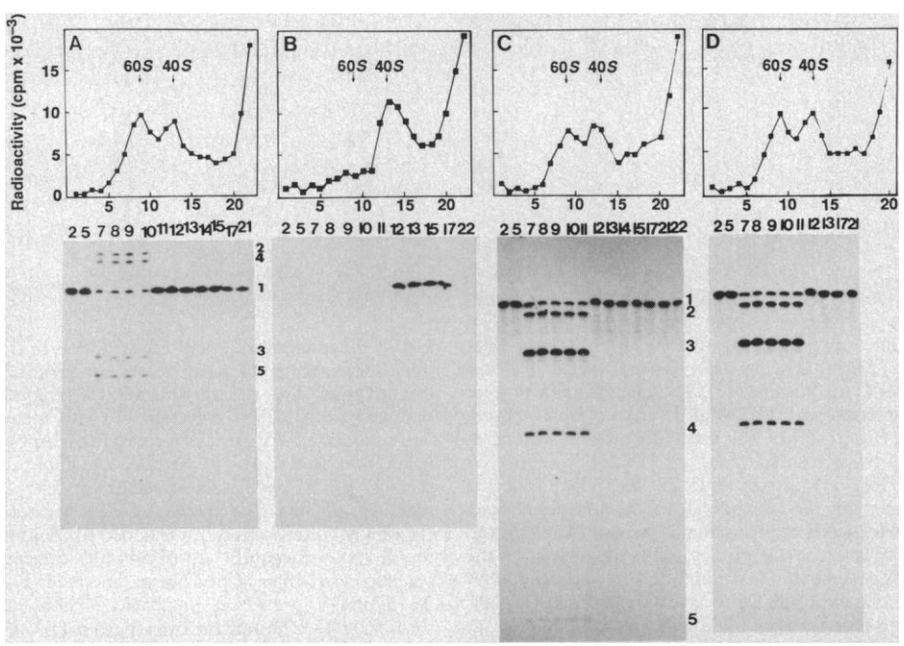

Fig. 4. Ribonucleoprotein complex analysis of the products of the in vitro splicing reaction in extracts from HIV-1–infected cells. Splicing reactions with SP6/HIV pre-mRNAs in the presence of (**A**) uninfected or (**B**) HIV-1–infected H9 extracts were performed as in Fig. 2 and immediately layered over 15 to 40% glycerol gradients as described (*17*). Fractions were collected and the nucleic acids extracted. The radioactivity (^{32}P) was determined by Cerenkov radiation (in counts per minute). The marker 60*S* and 40*S* ribosomal subunits (indicated by arrows) were run in a separate gradient. Sedimentation was from right to left. Splicing reactions with SP6/mouse insulin pre-mRNA incubated in the presence of (**C**) uninfected or (**D**) HIV-I–infected extracts were used as controls. The RNAs were analyzed on 4% (A and B) or 6% (C and D) 8*M*-urea polyacrylamide gels. The RNA species 1 to 5 (see Fig. 2) are indicated on the right of the autoradiograms in (A) and (C). The numbers on top of the autoradiograms indicate gradient fraction number.

its splicing of an HIV-1 pre-mRNA. This pre-mRNA contains an intron that is also part of the coding region for the envelope protein. Several studies (*24, 25*) reported cis-acting sequences that influence the levels of splicing of genomic retroviral RNAs that when removed inhibit splicing. It is very unlikely, however, that the inhibitory splicing effect we have shown was due to the lack of either intron-deleted sequences (Fig. 1) or HIV-1 upstream sequences, since the synthetic SP6/HIV pre-mRNAs were spliced normally in extracts from uninfected cells. A trans-regulatory modulation of RNA splicing has been postulated for a number of viral and cellular genes (*26, 27*). However, the demonstration of inhibitors of RNA splicing encoded by HIV-1 is without precedents in retroviruses or other systems. The HIV-1 viral-encoded inhibitors of RNA splicing in the *env*-coding region might be one of the control mechanisms operative in the switch from long latency to a cytopathic virus. The cytopathic effect of HIV-1 directly correlates with the expression of high levels of viral envelope proteins by an infected cell (*8, 16*). The regulatory control mechanism of viral RNA splicing affords the virus a means of rapidly responding with efficient production of viral structural proteins for virion assembly.

REFERENCES AND NOTES

1. I. S. Y. Chen, *Cell* **47**, 1 (1986).
2. A. G. Fisher *et al.*, *Nature* **320**, 367 (1986).
3. B. R. Cullen, *Cell* **46**, 973 (1986).
4. M. A. Muesing, D. M. Smith, D. J. Capon, *ibid.* **48**, 691 (1987).
5. B. M. Peterlin *et al.*, *Proc. Natl. Acad. Sci. U.S.A.* **83**, 9734 (1986).
6. A. Dayton *et al.*, *Cell* **44**, 941 (1986).
7. J. G. Sodroski *et al.*, *Nature* **321**, 412 (1986).
8. M. B. Feinberg, R. F. Jarret, A. Aldovini, R. C. Gallo, F. Wong-Staal, *Cell* **46**, 807 (1986).
9. S. K. Arya, C. Guo, S. F. Josephs, F. Wong-Staal, *Science* **229**, 69 (1985); W. C. Goh *et al.*, *J. Virol.* **59**, 181 (1986).
10. J. Sodroski, R. Patarca, C. Rosen, F. Wong-Staal, W. Haseltine, *Science* **229**, 74 (1985); A. Aldovini *et al.*, *Proc. Natl. Acad. Sci. U.S.A.* **83**, 6672 (1986).
11. C. A. Rosen *et al.*, *Cell* **41**, 813 (1985).
12. C. A. Rosen *et al.*, *Nature* **319**, 555 (1986).
13. J. Hauber, A. Perkins, E. P. Heimer, B. R. Cullen, *Proc. Natl. Acad. Sci. U.S.A.* **84**, 6364 (1987).
14. S.-Y. Kao, A. F. Calman, P. A. Luciw, B. M. Peterlin, *Nature* **330**, 489 (1987).
15. C. M. Wright, B. K. Felber, H. Paskalis, G. N. Pavlakis, *Science* **234**, 988 (1986).
16. M. R. Sadaie, T. Benter, F. Wong-Staal, *ibid.* **239**, 910 (1988).

16a. L. Ratner *et al.*, *Nature* **313**, 277 (1985).

17. G. Kaltwasser, S. Spitzer, C. J. Goldenberg, *Nucleic Acids Res.* **14**, 3687 (1986).
18. M. R. Green, *Annu. Rev. Genet.* **20**, 671 (1986).
19. S. M. Mount *et al.*, *Cell* **33**, 509 (1983).
20. A. Kramer *et al.*, *ibid.* **38**, 299 (1984).
21. D. Frendewey and W. Keller, *ibid.* **42**, 355 (1985).
22. P. J. Grabowski, S. R. Seiler, P. A. Sharp, *ibid.*, p. 345.
23. Y. D. Choi, P. J. Grabowski, P. A. Sharp, G. Dreyfuss, *Science* **231**, 1534 (1986).
24. L. H. S. Huang, J. Park, E. Gilboa, *Mol. Cell. Biol.* **4**, 2289 (1984).
25. C. K. Miller and H. M. Temin, *J. Virol.* **58**, 75 (1986).
26. J. R. Nevins and M. Wilson, *Nature* **290**, 113 (1981).
27. R. E. Breitbart *et al.*, *Cell* **41**, 67 (1985).
28. P. L. Wollenzien *et al.*, *Nucleic Acids Res.* **15**, 9279 (1987).
29. The nuclear extracts obtained from HIV-1–infected H9 cells were fractionated through blue-dextran agarose and DEAE-Sepharose. Approximately 60 mg of protein (2 ml) was loaded onto a 3-ml blue-dextran agarose column equilibrated with HGE [25 m*M* Hepes (*p*H 7.9), 10% glycerol, 0.1 m*M* EDTA] plus 0.1*M* KCl. The flow-through was collected and the column washed with five column volumes of HGE plus 0.1*M* KCl. The column was eluted in four fractions (2 ml) with HGE plus 0.6*M* KCl. The active fraction was recovered in the first two fractions. This fraction was dialyzed against HGE + 0.1*M* KCl and applied to a 1-ml DEAE-Sepharose equilibrated in HGE + 0.1*M* KCl. The column was washed with five column volumes of HGE + 0.1*M* KCl and eluted with HGE + 0.2, 0.3, and 0.5*M* KCl, in fractions of 1.5 ml. These fractions were dialyzed against HGE + 0.1*M* KCl to test their effects on in vitro splicing.

30. We thank F. Breakenridge and W. Parks for the HIV-1–infected cells; R. Voellmy, J. Patton, T. Malek, N. Fregien, and G. Conner for discussions; and A. Gatell for technical assistance. Supported by NIH grant AI-24479.

2 May 1988; accepted 15 July 1988

A Cineradiographic Analysis of Bird Flight: The Wishbone in Starlings Is a Spring

FARISH A. JENKINS, JR., KENNETH P. DIAL, G. E. GOSLOW, JR.

High-speed x-ray movies of European starlings flying in a wind tunnel provide detailed documentation of avian skeletal movements during flapping flight. The U-shaped furcula (or "wishbone," which represents the fused clavicles) bends laterally during downstroke and recoils during upstroke; these movements may facilitate inflation and deflation of the clavicular air sac. Sternal movements are also coupled with wingbeat, ascending and retracting on downstroke and descending and protracting on upstroke in an approximately elliptical pathway. The coupled actions of the sternum and furcula appear to be part of a respiratory cycling mechanism between the lungs and air sacs.

CURRENT UNDERSTANDING OF THE mechanisms of bird flight is based largely on conventional photography (*1*). The mechanics of a wing's musculoskeletal structure, however, can only be inferred by these techniques. The action of the shoulder girdle, which is obscured by plumage, has remained unresolved. Our analysis of radiographic films of birds in flight provides detailed data on the excursions of the bones in the wing and shoulder and demonstrates that the furcula (the "wishbone") acts as a spring.

European starlings (*Sturnus vulgaris*) were radiographed in both lateral and dorsoventral projections at 200 frames per second as they flew in a wind tunnel at air speeds of 9 to 20 m/s (20 to 45 mile/hour) (*2*). For descriptive purposes the wingbeat cycle as seen in x-ray films can be divided into four phases: (i) upstroke-downstroke transition (ii) downstroke, (iii) downstroke-upstroke transition, and (iv) upstroke. During the upstroke-downstroke transition, the longitudinal axis of the humerus comes to lie in a sagittal or nearly sagittal plane (Fig. 1A, top). Thereafter the wing protracts (that is, moves craniad); in this movement the angular intersection of the longitudinal axis of the humerus and the longitudinal body axis increases from an acute angle (Fig. 1A, bottom) to about 50°. As downstroke begins, the humerus is further protracted another 5° to 10° and the elbow and carpal joints extend. During the downstroke (Fig. 1, B and C) the humerus depresses some 110° but is maintained at a relatively constant angle (55° to 60°) with respect to the longitudinal body axis.

The downstroke-upstroke transition is characterized by humeral elevation and adduction and by nearly simultaneous flexion of the elbow and carplus.

During flight the shafts of the furcula are bent laterally during downstroke (Fig. 1, A through C, top) and recoil during upstroke (Fig. 1, D through A, top). The mean excursion of the dorsal ends of the furcula in four birds was 5.8 mm (SD, 1.0 mm), an increase of 47% over the resting distance, which averaged 12.3 mm (SD, 0.2 mm) (Fig. 2A). The minimum intrafurcular distance during flight averaged 12.9 mm (SD, 0.6 mm), and the average maximum intrafurcular distance was 18.7 mm (SD, 0.9 mm) (*3*). Furcular spreading begins as the distal end of the humerus moves craniad

F. A. Jenkins, Jr., and K. P. Dial, Department of Organismic and Evolutionary Biology and Museum of Comparative Zoology, Harvard University, Cambridge, MA 02138.
G. E. Goslow, Jr., Department of Biological Sciences, Northern Arizona University, Flagstaff, AZ 86011.